

Image Processing Algorithms for Digital Mammography: A Pictorial Essay¹

*Etta D. Pisano, MD • Elodia B. Cole • Bradley M. Hemminger, MS
Martin J. Yaffe, PhD • Stephen R. Aylward, PhD • Andrew D. A.
Maidment, PhD • R. Eugene Johnston, PhD • Mark B. Williams, PhD
Loren T. Niklason, PhD • Emily F. Conant, MD • Laurie L. Fajardo, MD
Daniel B. Kopans, MD • Marylee E. Brown • Stephen M. Pizer, PhD*

Digital mammography systems allow manipulation of fine differences in image contrast by means of image processing algorithms. Different display algorithms have advantages and disadvantages for the specific tasks required in breast imaging—diagnosis and screening. Manual intensity windowing can produce digital mammograms very similar to standard screen-film mammograms but is limited by its operator dependence. Histogram-based intensity windowing improves the conspicuity of the lesion edge, but there is loss of detail outside the dense parts of the image. Mixture-model intensity windowing enhances the visibility of lesion borders against the fatty background, but the mixed parenchymal densities abutting the lesion may be lost. Contrast-limited adaptive histogram equalization can also provide subtle edge information but might degrade performance in the screening setting by enhancing the visibility of nuisance information. Unsharp masking enhances the sharpness of the borders of mass lesions, but this algorithm may make even an indistinct mass appear more circumscribed. Peripheral equalization displays lesion details well and preserves the peripheral information in the surrounding breast, but there may be flattening of image contrast in the nonperipheral portions of the image. Trex processing allows visualization of both lesion detail and breast edge information but reduces image contrast.

Abbreviations: CLAHE = contrast-limited adaptive histogram equalization, HIW = histogram-based intensity windowing, MIW = manual intensity windowing, MMIW = mixture-model intensity windowing

Index terms: Breast radiography, 00.1215 • Images, display, 00.1215 • Images, processing, 00.1215 • Radiography, digital, 00.1215

RadioGraphics 2000; 20:1479–1491

¹From the Department of Radiology (E.D.P., B.M.H., S.R.A., R.E.J., M.E.B.), Lineberger Comprehensive Cancer Center (E.B.C.), and Department of Computer Science (S.M.P.), University of North Carolina, 101 Manning Dr, Chapel Hill, NC 27514-4226; the Department of Medical Imaging, University of Toronto, Ontario, Canada (M.J.Y.); the Department of Radiology, Thomas Jefferson University, Philadelphia, Pa (A.D.A.M.); the Department of Radiology, University of Virginia, Charlottesville (M.B.W.); the Department of Radiology, University of Pennsylvania, Philadelphia (E.F.C.); the Department of Radiology, Johns Hopkins University, Baltimore, Md (L.L.F.); and the Department of Radiology, Massachusetts General Hospital, Boston (D.B.K.). Recipient of a Certificate of Merit award for a scientific exhibit at the 1998 RSNA scientific assembly. Received October 5, 1999; revision requested November 12; final revision received February 7, 2000; accepted February 16. Supported in part by grant RO1-CA60193-05 from the National Cancer Institute; grant 282-97-0078 from the Office of Women's Health, Department of Health and Human Services; grant DAMD 17-94-J-4345 from the U.S. Army Medical Research and Material Command; grant 7289 from the Canadian Breast Cancer Research Initiative; and grants RO1-CA6019, RO1-CA75145-01A1, and RO1-CA60183 from the National Cancer Institute. **Address correspondence to E.D.P.** (e-mail: etpisano@med.unc.edu).

Introduction

The effectiveness of digital mammography in detection of breast cancer is currently under investigation. This imaging modality separates image acquisition and image display, thus allowing optimization of both.

In screen-film mammography, film serves as the medium for both image acquisition and display. Screen-film mammography has limited detection capability for low-contrast lesions in dense breasts. This limitation poses a problem for the estimated 40% of women with dense breasts who undergo mammography (1). In this population, diagnosis often requires additional imaging, which results in more radiation exposure for the patient. When additional images fail to provide useful diagnostic information, a decision must be made as to whether the suspicious regions require biopsy or short- or long-term follow-up. Because of the expense and risk associated with additional radiation exposure and surgery, any method of image presentation that increases the diagnostic conspicuity of lesions in breast tissue, especially in dense tissue, would be a significant advance.

Digital mammography systems, unlike screen-film mammography systems, allow manipulation of fine differences in image contrast by means of image processing algorithms. As a result, very subtle differences between abnormal and normal but dense tissue can be made more obvious. In this article, we illustrate the appearances produced by various image processing algorithms for display of digital mammograms and discuss how these algorithms may affect the ability of radiologists to interpret the images.

Selected Mammographic Lesions

The four cases used in this article to demonstrate the image processing algorithms were selected to show the range of types of mammographic lesions and the potential advantages and disadvantages of the different display algorithms. All of the digital mammograms shown in this article were acquired under research protocols approved

by the investigational review boards at the involved institutions.

The first case involves a partially obscured and partially circumscribed mass at screen-film mammography (Fig 1a), which proved to be a simple cyst at ultrasonography and needle aspiration. A digital mammogram of this case was acquired at the University of North Carolina, Chapel Hill, with a SenoScan full-field digital mammography unit (Fischer Imaging, Denver, Colo).

The second case involves two indistinct masses at screen-film mammography (Fig 2a, 2b). Both masses proved to be infiltrating ductal carcinomas with accompanying ductal carcinoma in situ at open surgical biopsy with needle localization. A digital mammogram of this case was acquired at Massachusetts General Hospital, Boston, with a Senographe 2000D full-field digital mammography system (GE Medical Systems, Milwaukee, Wis).

The third case involves a palpable, spiculated mass at screen-film mammography (Fig 3a, 3b), which proved to be an infiltrating ductal carcinoma with associated cribriform and solid-type ductal carcinoma in situ at open surgical biopsy. A digital mammogram of this case was acquired at the University of North Carolina with the Fischer Imaging unit.

The fourth case involves a pleomorphic cluster of calcifications at screen-film mammography (Fig 4a), which proved to be atrophic breast tissue at stereotactically guided core biopsy. A digital mammogram of this case was acquired at the University of Virginia, Charlottesville, with a Trex Digital Mammography System (Trex Medical, Danbury, Conn).

Overview of the Digital Mammography Systems

The Fischer Imaging unit produces images with a spatial resolution of 54 $\mu\text{m}/\text{pixel}$ and a matrix size of $3,072 \times 4,800$ pixels. The GE Medical Systems unit produces images with a spatial resolution of 100 $\mu\text{m}/\text{pixel}$ and a matrix size of $1,800 \times 2,304$ pixels. The Trex Medical unit produces images with a spatial resolution of 41 $\mu\text{m}/\text{pixel}$ and a matrix size of $4,800 \times 6,400$ pixels. The smaller

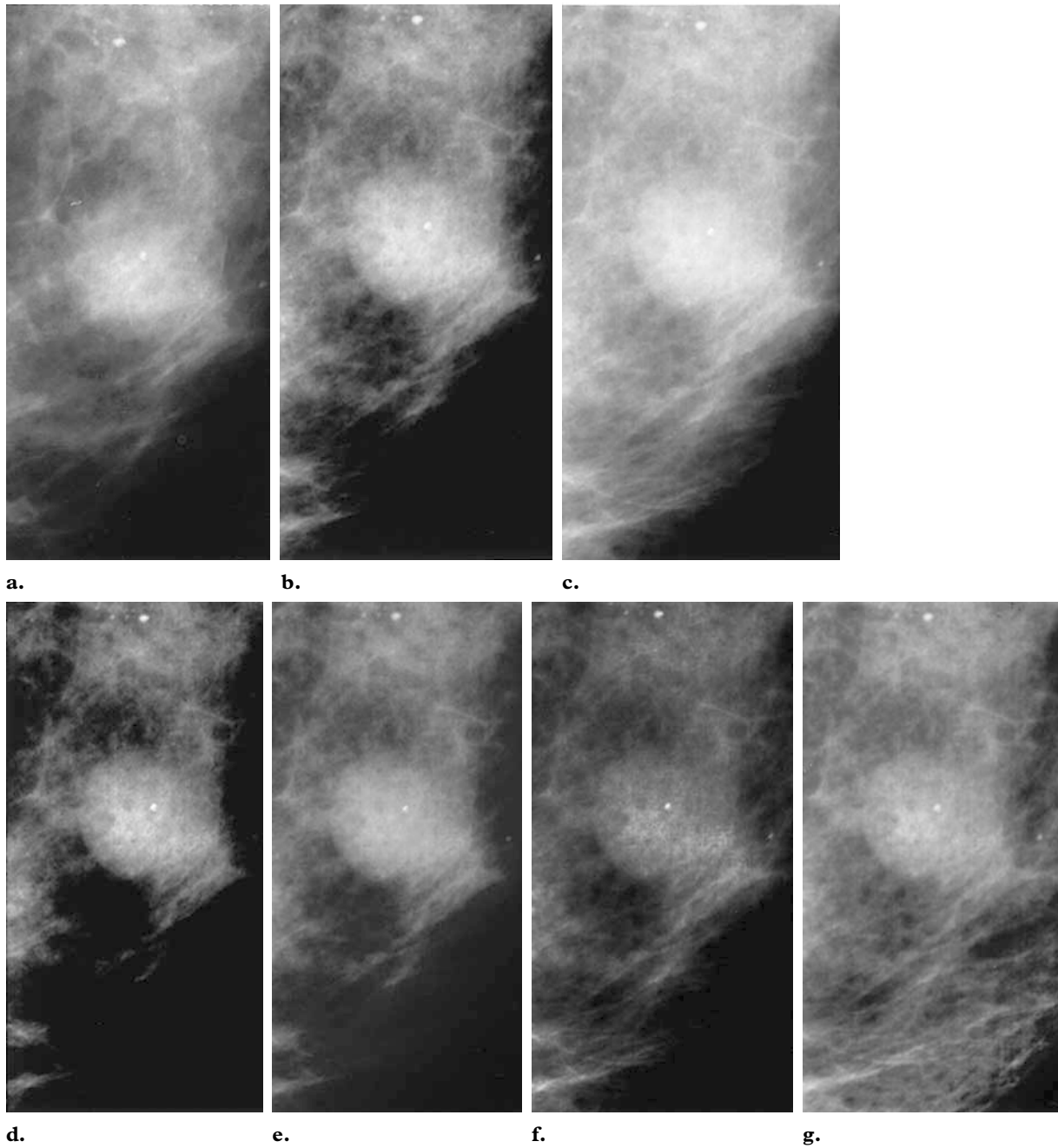
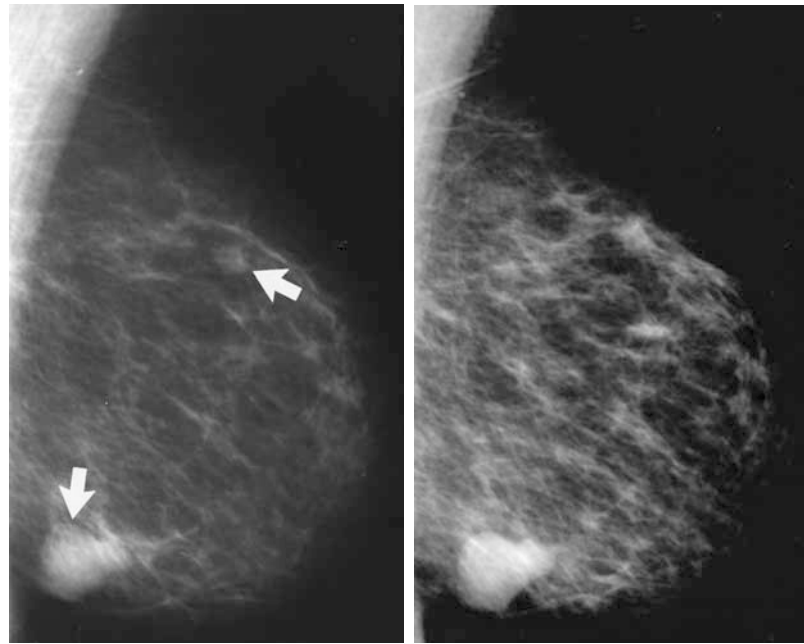


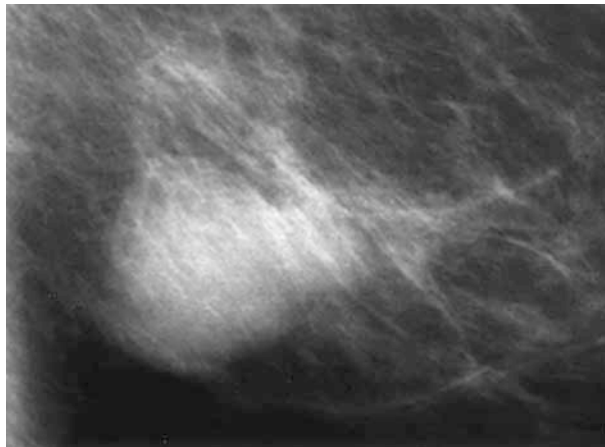
Figure 1. (a) Photographic magnification of a craniocaudal screen-film mammogram shows a cyst. (b–g) Photographic magnifications of a digital mammogram processed with MIW (b), HIW (c), MMIW (d), CLAHE (e), unsharp masking (f), and peripheral equalization (g) show the same lesion.

Figure 2. (a) Mediolateral oblique screen-film mammogram shows two masses (arrows), which both proved to be infiltrating ductal carcinomas with associated ductal carcinoma in situ at open surgical biopsy. (b) Photographic magnification of a shows the larger, inferior carcinoma. (c) Photographic magnification of a digital mammogram processed with MIW shows the larger lesion. (d) Digital mammogram processed with MMIW shows both cancers very well. (e) Photographic magnification of d shows the larger lesion. (f) Photographic magnification of a digital mammogram processed with unsharp masking shows the larger lesion. (Courtesy of D.B.K.)

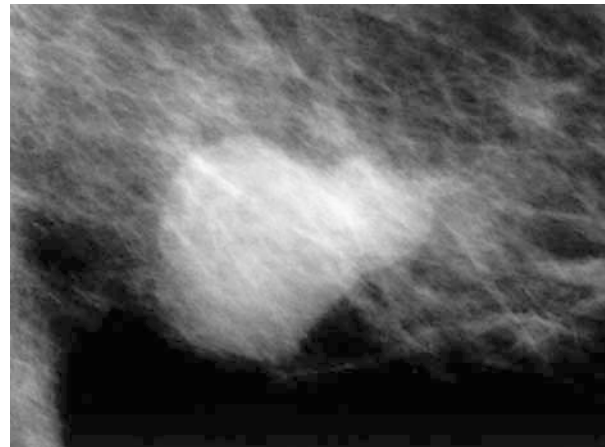


a.

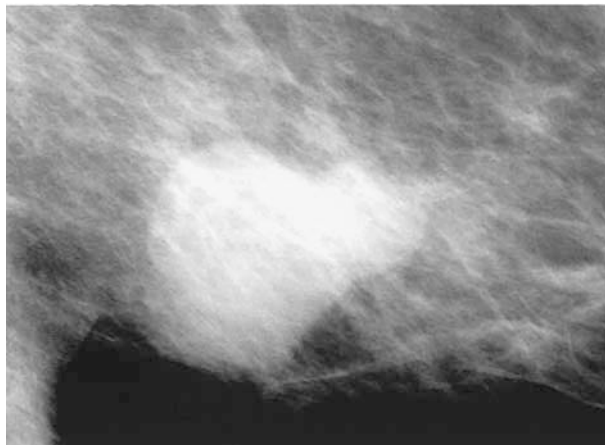
d.



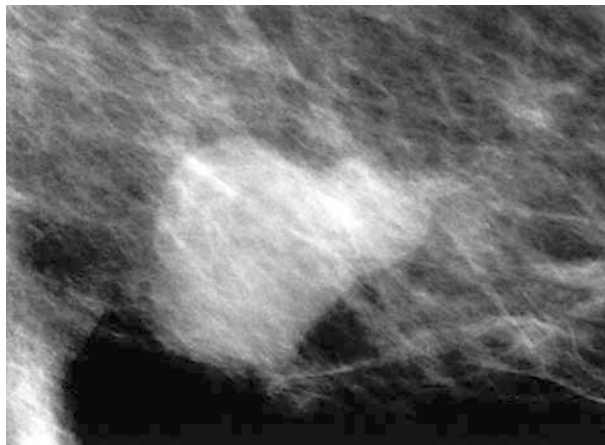
b.



e.



c.



f.

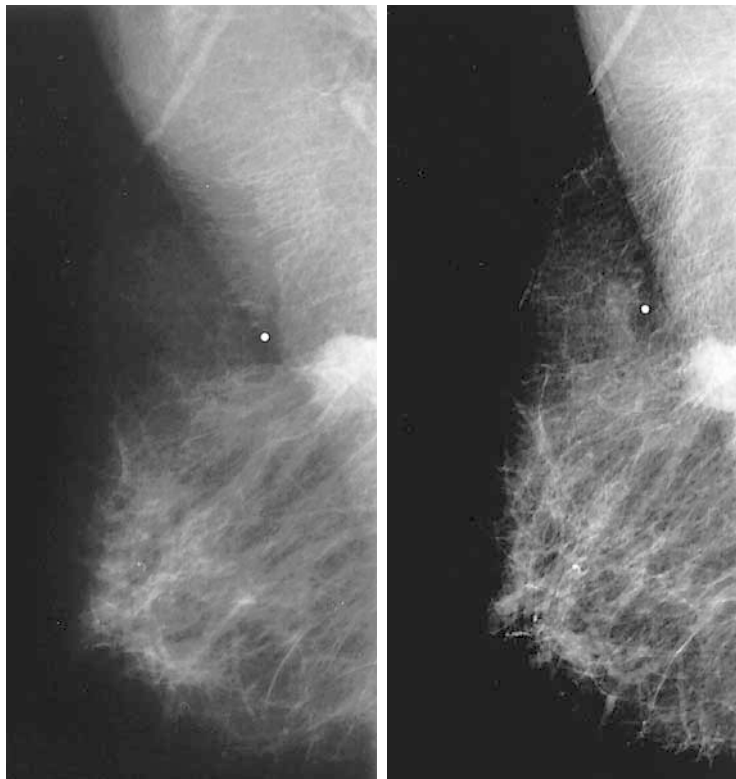
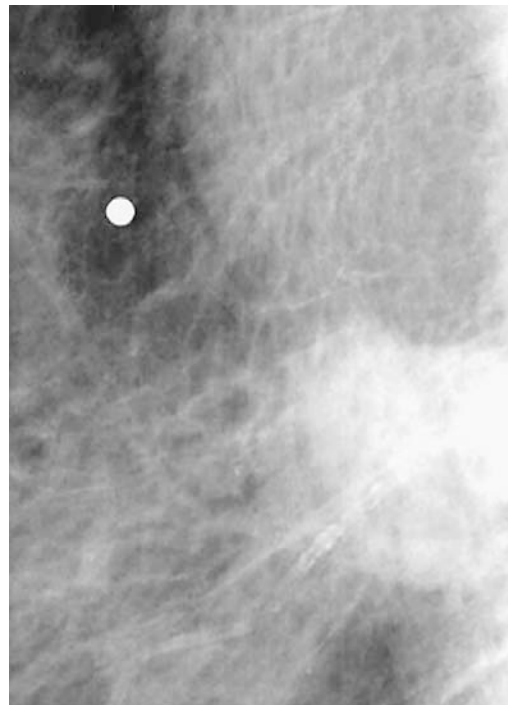
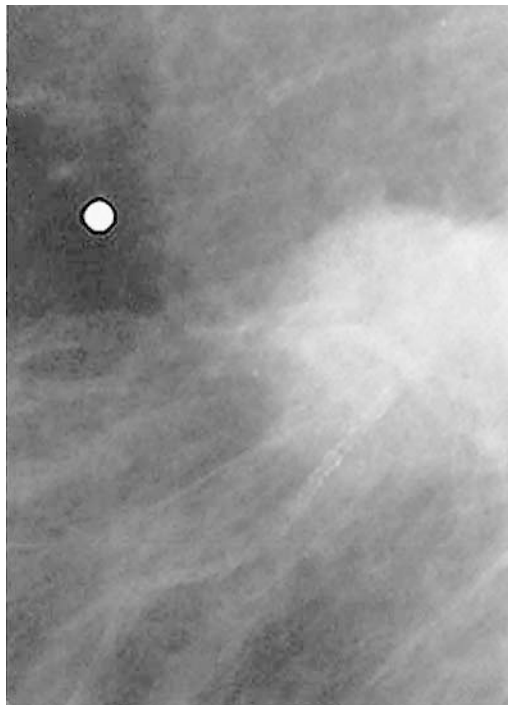


Figure 3. (a) Medi-
 olateral oblique
 screen-film mammo-
 gram shows a spiculated
 mass in the axillary por-
 tion of the breast, which
 proved to be an infiltrat-
 ing ductal carcinoma
 with associated cribri-
 form and solid-type
 ductal carcinoma in situ
 at open surgical biopsy.
 (b) Photographic mag-
 nification of a shows the
 lesion. (c, d) Digital
 mammogram processed
 with unsharp masking
 (c) and photographic
 magnification of c (d)
 show the lesion.

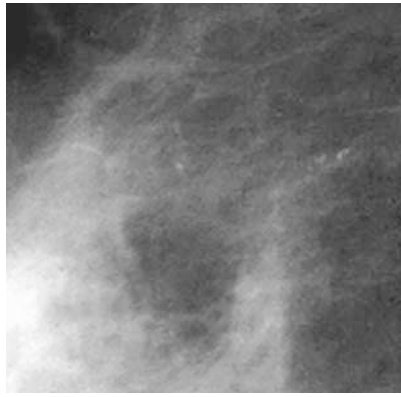
a.

c.

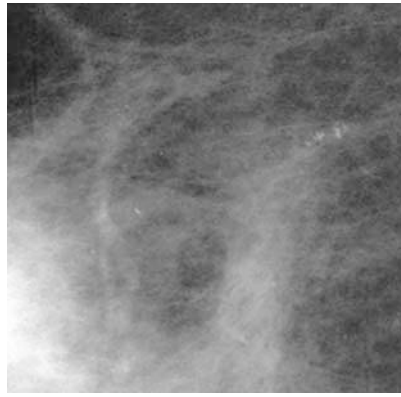


b.

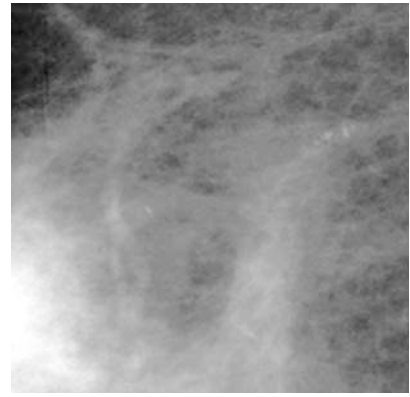
d.



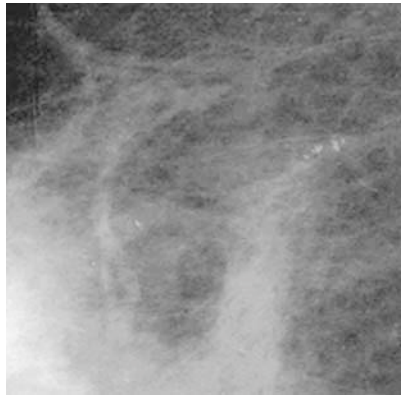
a.



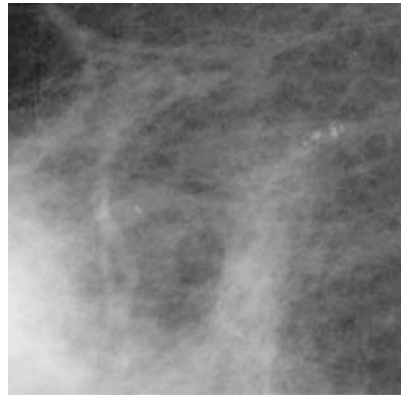
b.



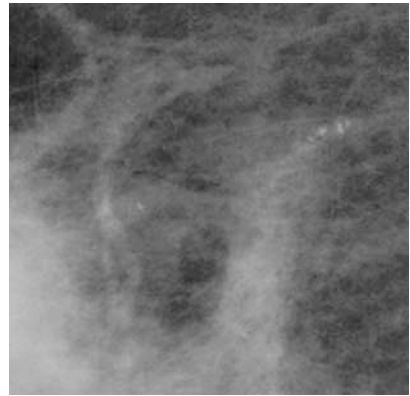
c.



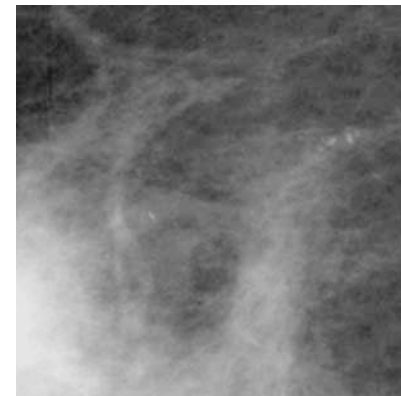
d.



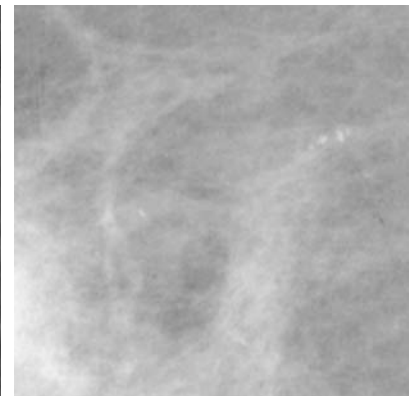
e.



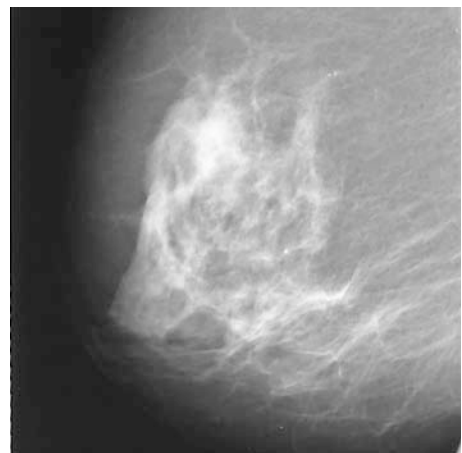
f.



g.



h.



i.

- ◀ **Figure 4.** (a) Photographic magnification of a mediolateral oblique screen-film mammogram shows a cluster of calcifications, which proved to be atrophic breast tissue at core biopsy. (b–g) Photographic magnifications of a digital mammogram processed with MIW (b), HIW (c), MMIW (d), CLAHE (e), unsharp masking (f), and peripheral equalization (g) show the clustered calcifications. (h, i) Digital mammogram processed with Trex processing (h) and photographic magnification of h (i) show the calcifications. (Courtesy of the University of Virginia and L.L.F.)

the number of micrometers per pixel, the smaller the features that can be measured in the image produced. As for contrast resolution, the Fischer Imaging unit offers 12 bits/pixel, whereas the GE Medical Systems and Trex Medical units offer 14 bits/pixel. Increasing contrast gradation provides the opportunity to distinguish finer and finer density differences between features in the image. However, it may not always be possible for a human observer to distinguish finer and finer gradations of gray owing to the limitations of visual perception and display devices. Detailed descriptions of the image acquisition hardware are provided elsewhere (2).

Image Processing Algorithms

Each manufacturer has developed image processing algorithms to use with its acquisition system. In addition, a number of algorithms have been developed by independent investigators for use with digital mammograms. The seven algorithms demonstrated in this article are manual intensity windowing (MIW), histogram-based intensity windowing (HIW), mixture-model intensity windowing (MMIW), contrast-limited adaptive histogram equalization (CLAHE), unsharp masking, peripheral equalization, and Trex processing.

Intensity windowing algorithms act on individual pixels within an image. A small portion of the full intensity range of an image is selected and then remapped to the full intensity range of the display device. This process allows selection of specific intensity values of interest. For example, intensity values that represent abnormal tissue and dense but normal tissue are selected to allow exaggeration of small differences in intensity values between the two objects, thus potentially increasing the conspicuity of any abnormal regions. The three versions of intensity windowing demonstrated in this article are MIW, HIW, and MMIW. These algorithms differ in how intensity values of interest are selected.

Manual Intensity Windowing

MIW was performed by an expert mammography technologist, who interactively adjusted the contrast levels as appropriate for each image using a

high-brightness monitor (model 1654; Orwin Associates, Amityville, NY) and an UltraSPARC 2200 workstation (Sun Microsystems, Mountain View, Calif). The goal of this algorithm is to manually reproduce the appearance of a screen-film mammogram.

Digital mammograms processed with MIW can be very similar to standard screen-film mammograms of the same patients (Figs 1b, 2c, 4b). In the second case, the center of the larger mass is very light on the image processed with MIW (Fig 2c). This appearance is due to the technologist's selection of a window that allowed visualization of both lesions in the image. Both lesions were obvious to her trained eyes. To keep the smaller lesion from appearing less obvious or even disappearing completely, she windowed the larger lesion so that it was slightly lighter than ideal.

This case points out the obvious limitation of this interactive windowing algorithm: It is operator dependent. A less experienced operator might choose different windows that could obscure some of the visible disease.

Histogram-based Intensity Windowing

HIW is a variant of intensity windowing. Intensity windowing allows a selected subrange of the image intensity values to receive the full contrast of the display device. All parts of the image with values outside the selected intensity window range are set to black (values below the minimum value of the intensity window range) or white (values above the maximum value of the intensity window range). HIW customizes standard intensity windowing by individually selecting the intensity window range for each image by statistically analyzing the histogram of each image, locating the "humps" or modes of the histogram, and determining which modes represent the different breast tissue types (fatty, dense, muscle) or other parts of the image (background, labels). From these known modes in the histogram, an

intensity window range is automatically selected on the basis of the percentile position within the composite breast tissue class (ie, fatty, dense, and muscle) that allows windowing over the overall breast tissue present in that patient (Fig 5).

For example, if the patient's breast is mainly fatty, the window selected will allow the full range of contrast across the part of the histogram representing the fatty portions of the breast. If the breast is mixed fatty and dense, the window will be selected on the basis of the portions of the histogram that represent those areas. In theory, this process should improve the detection of mammographic features in comparison with fixed intensity windowing, which cannot adapt to individual images. The adaptability of HIW to individual breast types makes it especially appropriate for digital mammograms because the breast tissue is always imaged with reasonable contrast, but the range of digital values containing the breast tissue can vary significantly depending on the acquisition parameters.

This automated windowing algorithm was used in the first and fourth cases (Figs 1c, 4c). In the case of the cyst, note the improved conspicuity of the lesion edge in the digital mammogram (Fig 1c) compared with that in the screen-film mammogram (Fig 1a). Part of the difference in the visibility of the lesion border and the accompanying benign calcifications is attributable to differences in positioning and compression. There is some loss of detail outside the dense parts of the HIW-processed image (Fig 1c) when compared with the screen-film image (Fig 1a) and the digital mammograms processed with other algorithms. This loss of detail might detract from use of this algorithm for screening.

Mixture-Model Intensity Windowing

MMIW provides region-specific intensity window settings for mammograms. It operates by automatically identifying the five major regions in a mammogram: background, uncompressed fat, compressed fat, dense tissue, and muscle. It identifies these regions using a combination of geometric (ie, gradient magnitude ridge traversal) and statistical (ie, Gaussian mixture modeling) techniques. Once these regions have been identified, their histograms can be selectively analyzed to determine region-specific intensity window settings. In our selected cases, MMIW was used to determine intensity window settings specific to the dense regions in the mammogram (3).

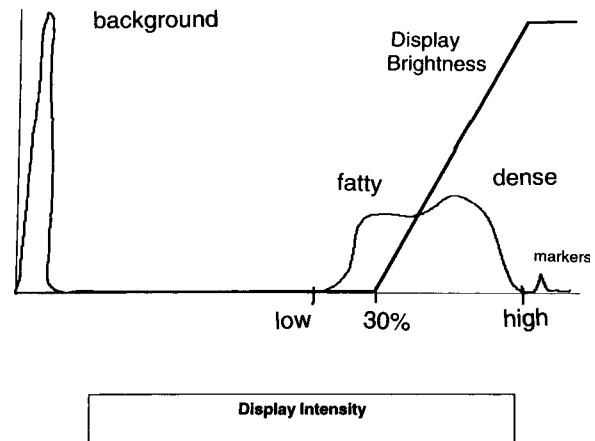
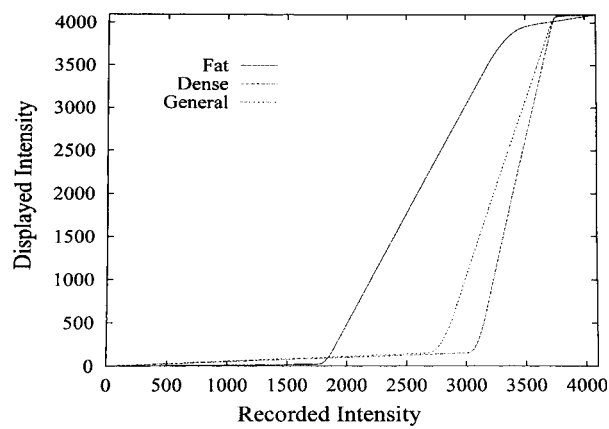
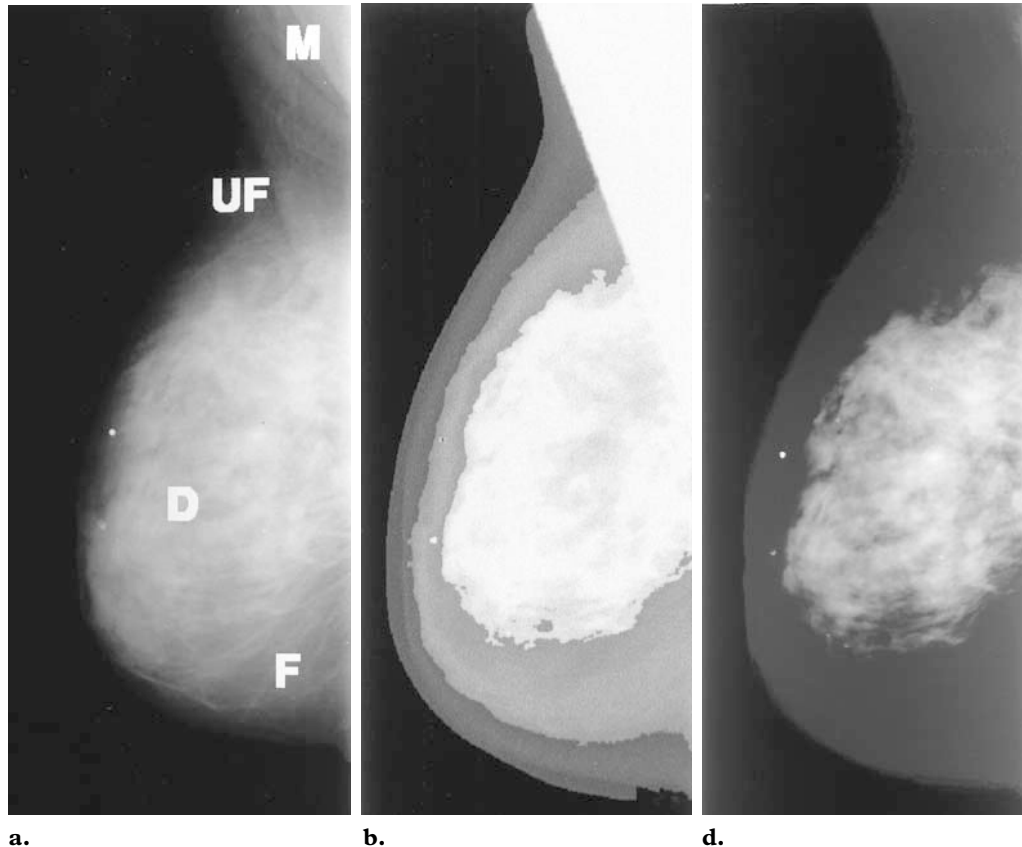


Figure 5. Histogram for a digital mammogram. The range of intensity values representing breast tissue is seen on the right. These are automatically recognized by HIW. HIW then chooses a display range based on this breast tissue range. In this example, a 30%–100% range is chosen. Then, the output range of the display device is mapped to the selected intensity window range (the 30% location maps to black, the 100% location maps to white).

The specific steps performed during MMIW are as follows: First, the major regions of a mammogram are labeled (Fig 6a). Since mammograms are formed by means of projection, these region labels reflect the prominent tissue present at that location, not the absolute quantities of the multiple tissues that affected x-ray absorption at each point. Second, the regions are segmented and the image is automatically cropped to reduce the portion of background (Fig 6b). With the regions identified, the intensity histogram of each region can be calculated. The mean and standard deviation of the intensities in each region are used to parameterize a sigmoidal intensity window function. These functions map recorded intensity to displayed intensity for each region (Fig 6c). Application of the dense region-specific intensity window function to the entire image produces the final processed image (Fig 6d). Each MMIW-processed image shown in this article was processed using its own MMIW-defined, dense region-specific intensity window function.

This algorithm enhances the visibility of the lesion borders against the fatty background (Figs 1d, 2d, 2e, 4d). However, the mixed parenchymal densities that abut the lesion are lost in some cases. This effect is most dramatic at the edges of the mammogram (Fig 2d). Clearly, if this type of statistical sampling of the image is used to determine an optimal intensity window, an additional algorithm that enhances the visibility of the periphery of the breast should be used to rescue information that is lost at the low-density subcutaneous regions of the breast.

Figure 6. Application of MMIW to digital mammograms. **(a)** Mediolateral oblique digital mammogram shows dense tissue (*D*), fat (*F*), pectoral muscle (*M*), and uncompressed fat (*UF*). The black area is the background. **(b)** Same image as in **a** after segmentation and cropping shows the muscle, dense tissue, compressed fat, and uncompressed fat portions of the image as different portions of the gray scale of the image. **(c)** Graph shows how the recorded intensity of the different regions in the image is mapped to the different displayed intensities in **d**. **(d)** Same mammogram as in **a** after automatic application of MMIW.



Both HIW and MMIW might be useful on a workstation. At the touch of a button, radiologists could request a processed digital mammogram that allows them to see through the densest portions of the breast. However, neither algo-

rithm would probably be acceptable for display of screening mammograms because information in the peripheral and fatty areas of the breast is not visible when these algorithms are applied.

Contrast-limited Adaptive Histogram Equalization

CLAHE is a special class of adaptive histogram equalization. Adaptive histogram equalization maximizes the contrast throughout an image by adaptively enhancing the contrast of each pixel relative to its local neighborhood. This process produces improved contrast for all levels of contrast (small and large) in the original image. For adaptive histogram equalization to enhance local contrast, histograms are calculated for small regional areas of pixels, producing local histograms.

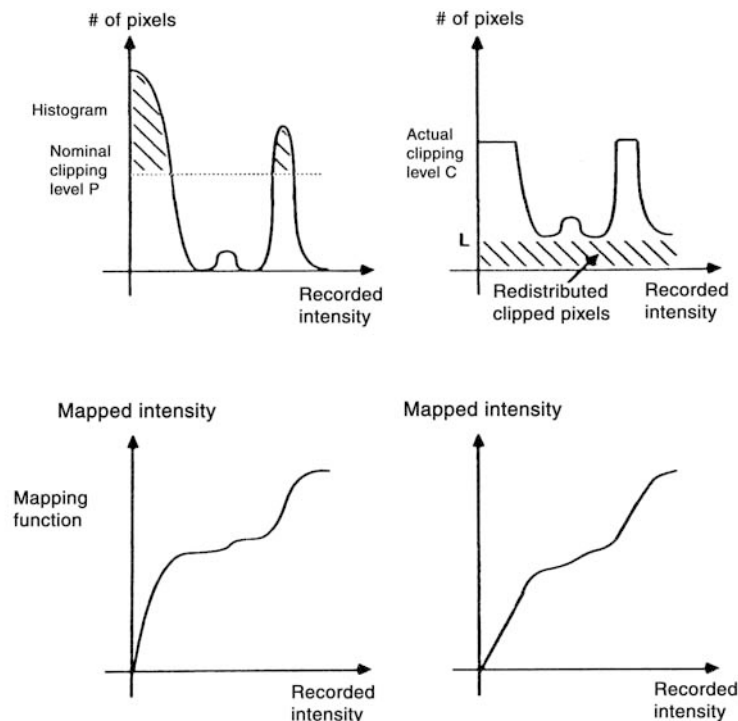


Figure 7. Clipping with CLAHE. Graphs show how CLAHE redistributes the mapped intensities of the pixels in an image.

These local histograms are then equalized or remapped from the often narrow range of intensity values indicative of a central pixel and its closest neighbors to the full range of intensity values available in the display.

CLAHE limits the maximum contrast adjustment that can be made to any local histogram (Fig 7). This limitation is useful so that the resulting image does not become too noisy. The size of the neighbor region is controlled by means of the region size parameter. Smaller regions can better enhance the contrast of smaller spatial scale structures. The CLAHE parameter settings (clip 4, region size 32 pixels squared) used in the sample digital mammograms shown in this article were selected on the basis of previous experiments (4). After CLAHE was applied, MIW was used so that the contrast of the resulting image more closely approximated that of standard screen-film mammograms.

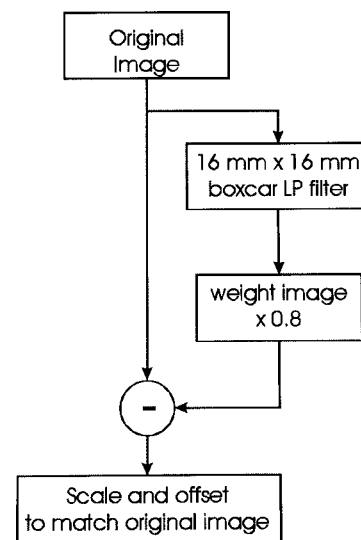


Figure 8. Application of unsharp masking. A weighted, low-pass (*LP*) filtered image is subtracted from the original image. For consistency in display, the data are then rescaled and an offset is added when necessary.

In digital mammograms processed with CLAHE, lesions appear obvious relative to the background and the image detail is very good (Figs 1e, 4e). However, there is obvious graininess in the images. This graininess is due to the enhanced visibility of both image signal and image noise with this algorithm. Again, this algorithm might be helpful in allowing radiologists to see subtle edge information, such as spiculation. It might degrade performance in the screening setting by enhancing the visibility of nuisance information that could simulate calcifications.

Unsharp Masking

With unsharp masking, a low-pass filtered version of the original image is created and the image values that result are subsequently multiplied by a weighting factor and subtracted from the original image (5). The final image preserves much of the detail of the original image, but large structures are presented with less contrast, thereby reducing the dynamic range required to display the image. In preliminary experiments,

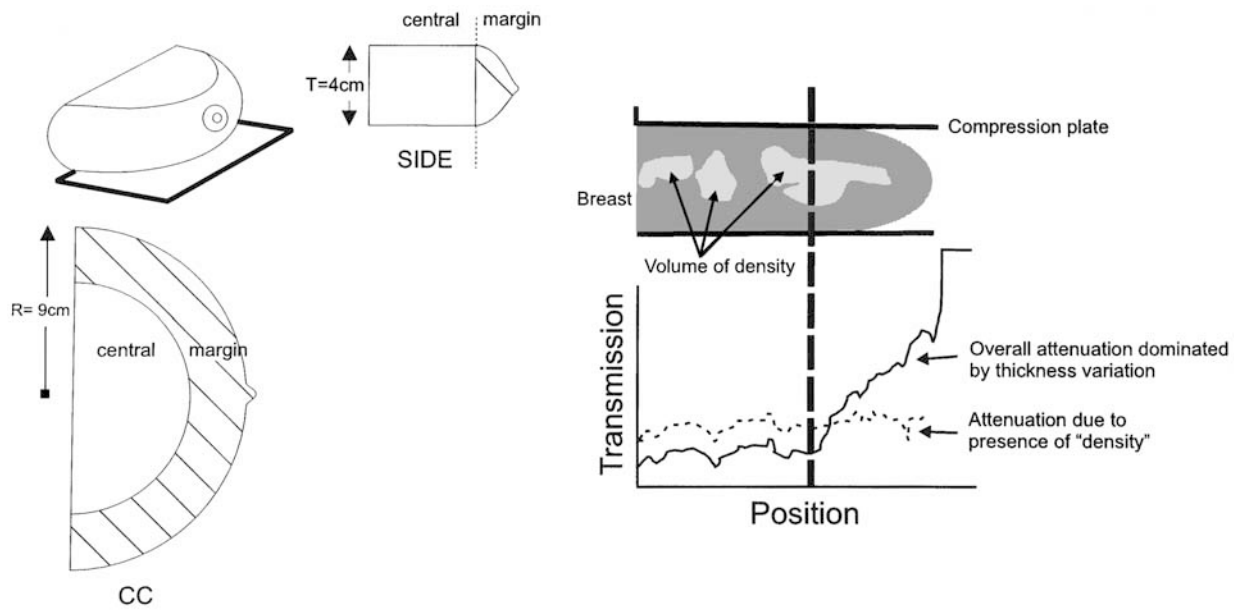


Figure 9. Effect of varied thickness of compressed breast tissue. Schematics of the compressed breast show that it consists of two regions: a central region of approximately uniform thickness and a margin where thickness varies. In the margin, variation in transmitted x-ray fluence occurs due to changes in both breast thickness and composition. CC = craniocaudal, R = radius, T = thickness.

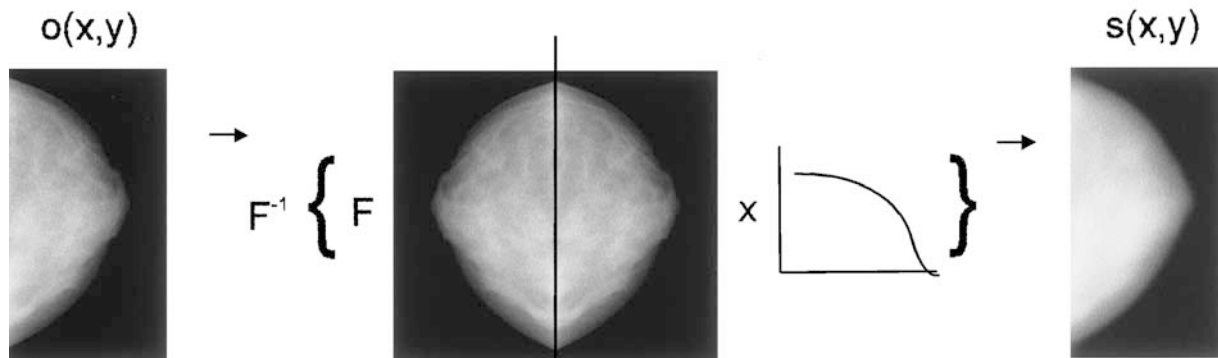
we tested a variety of low-pass filters using kernel sizes of 2–33 mm². In addition, a variety of weighting factors were tested. A boxcar filter with a window size of 16 mm² and a weighting factor of 0.8 was found to optimally compress dynamic range while preserving necessary structures in the breast and minimizing artifacts. A kernel size based on area was chosen so that comparison between manufacturers was possible despite differences in pixel size. The image data were then rescaled and an offset was added, as necessary, to approximately match the distribution of gray levels in the unprocessed and unsharp masked images (Fig 8). MIW was then applied to the resultant image to adjust the contrast to levels more closely approximating those of standard screen-film mammograms.

With unsharp masking, the sharpness of the borders of mass lesions is enhanced, as is the intended effect of this algorithm (Figs 1f, 2f, 3c, 3d, 4f). The spiculations in the third case are especially evident (Fig 3c, 3d). Of course, even an

indistinct mass can appear more circumscribed when this algorithm is applied (Fig 2f), obviously an undesirable outcome if this appearance were to lead to inappropriate patient follow-up instead of biopsy.

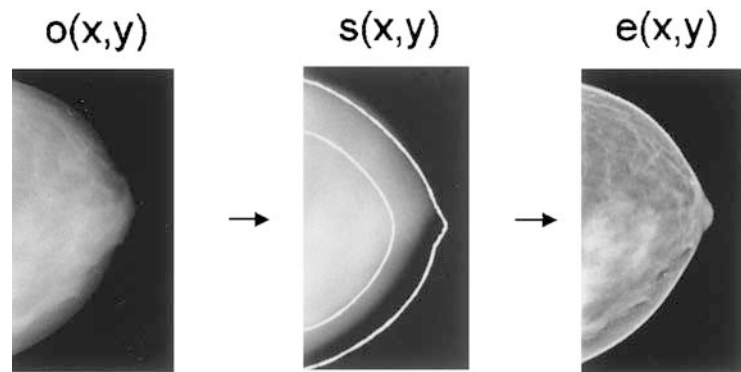
Peripheral Equalization

There are variations in the thickness of breast tissue under compression. The outer edges of the breast, which are thinner than the interior, are typically overpenetrated by x rays at image acquisition. Although a digital acquisition system should have adequate dynamic range to record this information precisely, the limited latitude of the laser film necessitates a compromise in image display. If the central parenchyma is presented with high contrast, then the peripheral tissue will appear very black on the film and may be difficult to distinguish visibly from the black film background (Fig 9).



a.

Figure 10. Peripheral equalization. (a) A smoothed representation of the image, $s(x,y)$, is obtained with a low-pass filtering operation. The low-pass filter (shown schematically in one dimension) is a first-order Butterworth filter with a cutoff frequency of 0.05 cycles per millimeter. (b) Overview of the thickness equalization processing technique. For each point in the margin, the smoothed image is used to determine a correction factor.



b.

Peripheral equalization enhances visualization of tissue located near the periphery of the breast (6,7). In peripheral equalization, a low-pass spatial filter is applied to the image to create a blurred “mask” that represents primarily the coarsest variations in signal, which are related to variations in breast thickness. This mask is scaled from 0 to 1, and the mammogram is divided by means of the mask values on a pixel-by-pixel basis (Figs 10a, 10b, 11). The algorithm is constrained to act only on pixels that lie within the breast and where the breast thickness is changing. There are also constraints placed on the total amount of enhancement to avoid disturbing artifacts at the skin line. The result is that the digital values of pixels located near the periphery are changed so that the absolute intensities of the image become “flatter” across the mammogram.

The local contrasts between pixels located near each other, which represent compositional variations in tissue, are not suppressed. In fact, because the part of the dynamic range of the film required to represent thickness changes is no longer required, it is now possible to increase the overall contrast of the image if desired. For the images shown in this article, after peripheral equalization was applied, MIW was used to adjust the resultant image contrast.

Details of both masses and calcifications are well depicted in images processed with peripheral equalization (Figs 1g, 4g). In addition, the peripheral information in the surrounding breast is preserved (Fig 1g). This algorithm might be effective in the screening setting because it preserves image features in all breast locations. However, there does appear to be some flattening of image contrast in the nonperipheral portions of mammograms when this algorithm is applied.

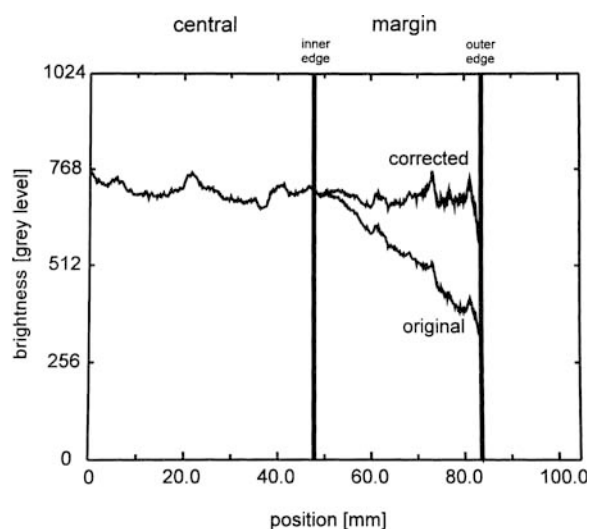


Figure 11. Profile of brightness as a function of position across a line of the original and corrected images. The vertical lines identify the margin. Note the reduction in the range of levels in the corrected data as a result of the adjustment in the margin.

Trex Processing

Trex processing was developed by Trex Medical for use with the Trex Digital Mammography System. This method uses a form of histogram-based unsharp masking.

The algorithm allows visualization of both lesion detail and breast edge information (Fig 4h, 4i). However, there is some reduction of image contrast, which is evident when a Trex-processed version is compared with other processed versions of the same image.

Conclusions

It is obvious from the images shown in this article that different digital image processing algorithms are likely to be useful for different tasks. Characterization of lesions and screening will most probably require a uniquely adapted image processing algorithm to provide the best presentation for visualization of different image features. In addition, different types of lesions, masses, and calcifications might benefit from specifically

tailored algorithms. Such tailoring will not be easily achieved unless the current method of displaying mammograms on film is replaced by a softcopy display system.

Given the added costs, the efficacy of digital mammography will ultimately depend on improved diagnostic accuracy over that of conventional screen-film mammography. Development and assessment of image processing methods that allow detection and characterization of individual lesion types will be instrumental in the acceptance of this new technology.

Acknowledgments: The unsharp masking algorithm was provided by A.D.A.M.; the peripheral equalization algorithm was provided by M.J.Y. and Gordon Mawdsley, PhD, University of Toronto, Ontario, Canada.

References

1. Shtern F. Digital mammography and related technologies: a perspective from the National Cancer Institute. *Radiology* 1992; 183:629–630.
2. Feig SA, Yaffe MJ. Current status of digital mammography. *Semin Ultrasound CT MR* 1996; 17: 424–443.
3. Aylward SR, Hemminger BM, Pisano ED. Mixture modeling for digital mammogram display and analysis. In: Karssemeijer N, Thijssen M, Hendriks J, van Erning A, eds. *Digital mammography* Nijmegen, 1998. Dordrecht, the Netherlands: Kluwer Academic, 1998; 305–312.
4. Pisano ED, Zong S, Hemminger BM, et al. Contrast limited adaptive histogram equalization image processing to improve the detection of simulated spiculations in dense mammograms. *J Digit Imaging* 1998; 11:193–200.
5. Chan HP, Vyborny CJ, MacMahon H, et al. Digital mammography ROC studies of the effects of pixel size and unsharp-mask filtering on the detection of subtle microcalcifications. *Invest Radiol* 1987; 22: 581–589.
6. Byng JW, Critten JP, Yaffe MJ. Thickness equalization processing for mammographic images. *Radiology* 1997; 203:564–568.
7. Bick U, Giger ML, Schmidt RA, Nishikawa RM, Doi K. Density correction of peripheral breast tissue on digital mammograms. *RadioGraphics* 1996; 16:403–411.